Available online at www.sciencedirect.com

ScienceDirect

Procedia Structural Integrity 28 (2020) 1846–1855

Structural Integrity Procedia

www.elsevier.com/locate/procedia

1st Virtual European Conference on Fracture

Fatigue Crack Growth Model Incorporating Surface Waviness For Wire+Arc Additively Manufactured Components

Kaveh Samadian[a,b*], Wim De Waele[a]

[a] *Ghent University, Faculty of Engineering and Architecture, Department of Electromechanical, Systems and Metal Engineering, Laboratory Soete, Technologiepark 46, 9052 Zwijnaarde, Belgium,*
[b] *SIM, Technologiepark 48, 9052 Zwijnaarde, Belgium*

Abstract

Wire+Arc additive manufacturing, due to its high deposition rate, is particularly suited for the construction and repair of large-scale components. For the very same reason, however, an important drawback of this process is the pronounced surface waviness. This waviness introduces multiple adjacent peaks and valleys at the component surface, acting as stress concentration sites which can undermine the fatigue performance. In the present work, the authors propose a framework to model fatigue crack propagation considering the effect of waviness at the component surface. The growth model takes the stress concentration factor as input and incorporates it in a two-fold crack propagation model of a planar flaw. The fracture mechanics based growth models are developed based on El Haddad's short crack model and the Paris equation for long crack propagation. The effects of stress concentration sites are firstly considered by modifying the short crack propagation parameters. Secondly by introducing a new crack length dependent stress intensity factor threshold, surface waviness is incorporated in the transition from short crack into long crack regime. The results show that short cracks originating from an as-built WAAM surface grow faster as compared to their counterparts originating from machined surfaces.

Keywords: Additive manufactering; WAAM; Fatigue; crack propagation; Short crack growth; Waviness

* Corresponding author. Tel.: +32 9 331 04 84; fax: +32 9 331 04 90.
E-mail address: Kaveh.Samadian@UGent.be

10.1016/j.prostr.2020.11.008

1. Introduction

Additive manufacturing (AM) as an alternative to conventional subtractive manufacturing of metals, has gained lots of interest during recent years. Its capability to manufacture complex shapes through layer by layer deposition allows for higher design flexibility and significant weight reduction. With a comparatively high buy-to-fly ratio Wire+Arc Additive Manufacturing (often referred to as WAAM) is a promising technique for fabrication and repair of industrial components, Cunningham et al. (2018). Due to its high energy efficiency, WAAM using either gas metal arc welding (GMAW) or gas tungsten arc welding (GTAW) processes is more desirable for large components. However, due to the very same reason, Wire+Arc components have lower accuracy in dimension and surface waviness and thus normally require post-process machining. Even if a sufficient accuracy can be achieved in as-built parts by optimizing the process parameters and printing strategy, the waviness resulting from the deposition of various weld passes can adversely affect the mechanical properties, particularly the fatigue performance.

Failure under cyclic loading (i.e. fatigue) is a substantial risk for metallic AM components in various applications, Stephens et al. (2000). As such, the poor surface quality of AM as-built components normally necessitates post-processing such as milling. Post-deposition machining, however imposes extra costs, often it is not feasible for the entire component and it can nullify some of the AM advantages like optimized designs. Therefore, an optimized post-processing treatment, in which milling can be prioritized for critical locations, is desired. Having a clear and profound understanding of the effect of surface waviness on fatigue performance can significantly contribute toward formulation of such a procedure.

Surface profile can be divided into roughness, which contains higher frequency waves, and waviness, which contains lower frequency waves. Both contributions basically consist of multiple adjacent peaks and valleys, of which the valleys can act as stress raiser micro-notches stimulating crack initiation. Material in close proximity to the valleys on the surface experiences higher stresses than the nominal applied stress. In most manufacturing processes, including AM techniques, surface waviness is negligible. Therefore many attempts have been made to find a correlation between surface roughness and fatigue behavior, e.g. Ås et al. (2008), Gong et al. (2014), Singh et al. (2019), Solberg et al. (2019), Zhang and Fatemi (2019). The effect of surface roughness on fatigue behavior is considered through surface parameters like the roughness value R_a which represents a general topography context averaged over the entire surface. A surface with a higher R_a value is rougher and therefore supposed to experience higher stress concentrations and, consequently, demonstrating lower fatigue resistance. Although this parameter has been used to predict the fatigue behavior by amongst others Uzan et al. (2017) and Wycisk et al. (2014), it cannot adequately describe the critical effects on the crack initiation process related to the micro-notches on the surface, since R_a is an average parameter Novovic et al. (2004). Therefore, aiming at a more accurate quantification of the effect of surface roughness on fatigue, researchers have used other surface parameters like R_v, R_t, R_z and their combinations, e.g. Edwards and Ramulu (2014), Franco and Sinatora (2015), Masuo et al. (2018), Novovic et al. (2004). Although these approaches have shown to be capable of correlating surface roughness and fatigue behavior, there are still some shortcomings. For instance, when surface irregularities fall in the range of waviness, which is the case for the WAAM process, there is no evidence that these parameters are suitable for fatigue behavior prediction.

To achieve a more comprehensive model for surface irregularities, an alternative approach has been based on modeling the valley as a notch. To do so, the stress concentration factor of the notch should be determined either using geometrical formulas, for instance those suggested by Neuber (1946), Arola and Williams (2002) and Yang et al. (2018), or by using finite element simulations. As an example of the latter case, Suraratchai et al. (2008) used a fracture mechanics based approach to simulate the most critical valley as a notch and calculate its growth along the surface and in depth direction considering the effect of stress raisers at the surface. Dirisu et al. (2020) studied the effect of compressive residual stress on fatigue behavior of WAAM mild steel components. They considered the effect of stress concentration factors due to the surface waviness as a function of depth (α) and radius (ρ) of the notch.

Although these researches provided an illuminating insight on the effect of surface finish on the fatigue behavior (S-N curve) in a general context, there is still considerable ambiguity about crack growth behavior under the influence of surface roughness and waviness.

In the present paper the authors present a model to incorporate the effect of surface waviness on fatigue crack growth of WAAM components considering both short and long crack growth regimes.

2. Extraction of stress concentration factor from surface waviness

The effects of surface waviness are often considered in terms of a stress concentration similar to the notch effect. The stress concentration factor K_t is defined as the ratio of the maximum stress at the notch, denoted a 'valley' in the case of surface waviness, and the nominal applied stress. To calculate the stress concentration factor, a 2D finite element (FE) model has been employed in this work. To build the geometrical model, first a white light interferometer has been used to measure the surface profile of a WAAM component (see Fig.1-a). The measurement data consists of multiple lines of two dimensional coordinates. The x coordinate is the position along the length of the specimen and the y coordinate quantifies the height of the surface irregularities. The mesh size of the numerical model was set to be 0.01 mm, following a convergence study. To reduce computation time, the model is divided into three regions of which only the top region (surface) has a very fine 0.01 mm mesh size. The other regions gradually reduce in mesh size, as can be seen in Fig.1-b. The following boundary conditions are used: at one vertical edge all nodes are fixed and symmetrical conditions apply at the bottom horizontal edge. Load is introduced as uniform stress at the opposite vertical edge.

Using the stress output of the FE model, the stress concentration factor at the valleys is calculated using the "Theory of Critical Distances" developed by Taylor (2008). The stress averaged over a semi-circular area with radius 0.1 mm at the bottom of each valley is used. It is insufficient to only derive the maximum stress at one element at the critical valley, since this single value might be significantly affected by the finite element mesh size. For each valley the stress concentration factor is calculated as the ratio of the averaged stress to the nominal stress and the maximum ratio is defined as K_t which will be used in the analytical framework for fatigue crack growth calculations.

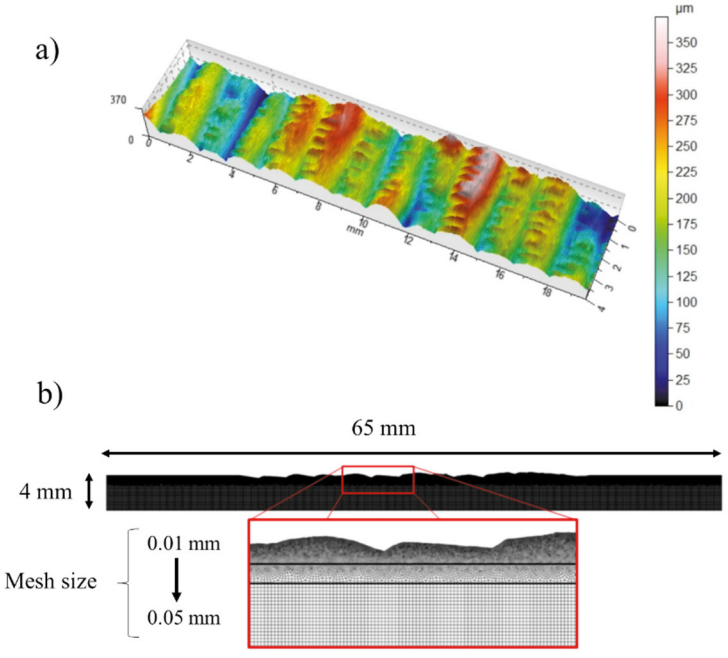

Figure 1: a) Surface profile of a WAAM component measured by white light interferometry, b) FE model of the as-built surface.

As shown by Suraratchai et al. (2008) an inverse relationship between the stress concentration factor K_t and the plain fatigue limit of the material exists. Therefore, the plain fatigue limit of a wavy surface ($\Delta\sigma_0^R$) scales inversely with K_t compared to the plain fatigue limit of a smooth machined surface ($\Delta\sigma_0$).

$$\Delta\sigma_0^R = \frac{\Delta\sigma_0}{K_t} \tag{1}$$

3. Theoretical background on fatigue crack propagation

The common approach to express fatigue crack growth, based on Linear Elastic Fracture Mechanics (LEFM), is the Paris-Erdogan equation:

$$\frac{da}{dN} = C\Delta K^m \tag{2}$$

Where a is the crack length, N is the number of cycles, ΔK is the stress intensity factor range and C, m are material specific parameters.

This approach is valid as long as LEFM conditions are maintained, determined by the magnitude of the stress and the ratio of the plastic zone size to the crack length. The applicability of LEFM can be debatable once the operating stress levels are too high, developing excessive plasticity, or when the crack size is small compared to either the plastic zone size or microstructural dimensions, Stephens et al. (2000). As such, short cracks will exhibit a growth regime which is significantly different from what would be expected based on the Paris-Erdogan equation. Kitagawa and Takahshi (1976) presented a diagram (often referred to as KT diagram) to describe the behavior of short cracks, as schematically shown in Fig.2 in which stress range ($\Delta\sigma$) and crack length (a) are depicted. The line labeled as A:A defines the long crack stress intensity factor threshold (ΔK_{th}) representing the combinations of stress range and crack length according to equation 3, below which a crack should not grow according to LEFM.

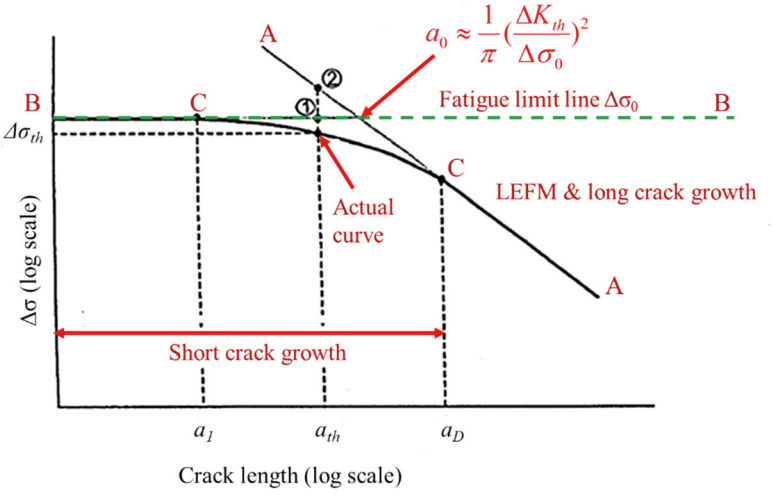

Figure 2: Schematic Kitagawa-Takahashi diagram.

$$\Delta K_{th} = \gamma\Delta\sigma\sqrt{\pi a} \tag{3}$$

Where a is crack length, $\Delta\sigma$ is the corresponding stress range threshold (based on LEFM) and γ is the shape factor. The horizontal line (B:B) represents the fatigue limit, below which fatigue life of an unnotched specimen is theoretically infinite. The regime of short crack propagation arises between certain crack lengths, a_1 and a_D in Fig.1, where experimental work has shown to diverge from these two theoretical lines, El Haddad et al. (1979a). On the segment

C:C of the "actual curve", a_1 defines the shortest crack length which is significant enough to decrease the fatigue limit and a_D defines the crack size at which the short crack effect on LEFM analysis diminishes. Therefore, for an arbitrary crack length (a_{th}), the actual stress range threshold ($\Delta\sigma_{th}$) is less than the stress range either suggested by the fatigue limit (point 1 in Fig.2) or what is predicted by LEFM in equation 2 based on long crack growth (point 2 in Fig.2). This condition, which holds true up to a crack length equal to a_D, causes crack growth below the long crack stress intensity factor threshold (ΔK_{th}) and below the fatigue limit, and consequently leads to non-conservative life prediction based on LEFM and/or fatigue limit.

Various studies have demonstrated that not only short cracks grow at values of ΔK below the long crack threshold, but also they can have significantly higher crack growth rate compared to the corresponding growth rate of a long crack with the same ΔK. Short cracks can be categorized into microstructurally and physically short cracks. The former category consists of cracks approximately smaller than 10 times a grain size and can be influenced substantially by microstructure, Irving and Beevers (1974). The growth of microstructurally short cracks normally violates the assumptions of continuum mechanics and LEFM, because of inhomogeneity and anisotropy at small microstructural scale. Physically small cracks are a category of cracks which normally don't violate LEFM limitations and are typically shorter than 1 or 2 mm. These cracks still grow at faster rates than long cracks subjected to the same nominal crack driving force and have lower ΔK_{th}.

One of the most acknowledged models to describe the asymptotic behavior of short cracks was proposed by El Haddad et al. (1979b). He proposed a stress intensity factor for a crack of length a in which the actual crack length is increased by a length constant a_0 to account for the behavior of very small cracks. By applying this to the long crack stress intensity factor threshold (ΔK_{th}), equation 4 can be derived:

$$\Delta K_{th} = \gamma \Delta\sigma \sqrt{\pi(a + a_0)} \tag{4}$$

For infinitely small cracks, it can be assumed that the stress range threshold ($\Delta\sigma$) approaches the plain fatigue limit $\Delta\sigma_0$:

$$\lim_{a\to 0} \Delta\sigma = \Delta\sigma_0 = \frac{1}{\gamma}\frac{\Delta K_{th}}{\sqrt{\pi a_0}} \tag{5}$$

Combining equations 4 and 5 results in the most used form of the crack length dependent stress intensity factor range threshold (ΔK_{th}) by El Haddad:

$$a_0 = \frac{1}{\pi}\left(\frac{\Delta K_{th}}{\gamma \Delta\sigma_0}\right)^2 \tag{6}$$

The critical defect length a_D can be related to El Haddad's intrinsic length a_0 by:

$$a_D = \frac{a_0}{\gamma^2} \tag{7}$$

The modified El Haddad equation for the stress intensity factor range threshold can be rewritten in its most common form:

$$\Delta K_a = \Delta K_{th} \frac{\sqrt{a}}{\sqrt{a + a_0}} \tag{8}$$

4. Unified crack growth model

The unified model for crack propagation considers both short and long crack propagation, with crack propagation occurring simultaneously along the surface and in through thickness direction. It is hypothesized that surface waviness will affect both directions differently. Crack growth along the surface (c-direction in Fig.3) remains in the region of increased stress and will be modeled by imposing a stress concentration factor K_t to the nominal applied stress range.

Crack growth in the through thickness direction (a-direction in Fig.3), is treated differently. Consider a short crack initiating at a valley of surface waviness; this crack will grow through a region of raised stress influenced by surface waviness. During its growth it will gradually leave this high stress region and the surface waviness effect will diminish. Once the crack length reaches a critical length, transition to the long crack propagation behavior occurs and it is hypothesized that this transition occurs outside of the by surface waviness affected region. As such, it can be hypothesized that a larger crack (in a-direction) is less affected by surface waviness and its growth is dictated more by the nominal applied stress range. In conclusion, since surface waviness only affects the region in close proximity to the surface, only the short crack propagation behavior in through thickness direction will be directly affected by surface waviness. Recall that the crack growth in surface direction, unlike through thickness direction, is hypothesized to be continuously affected by K_t.

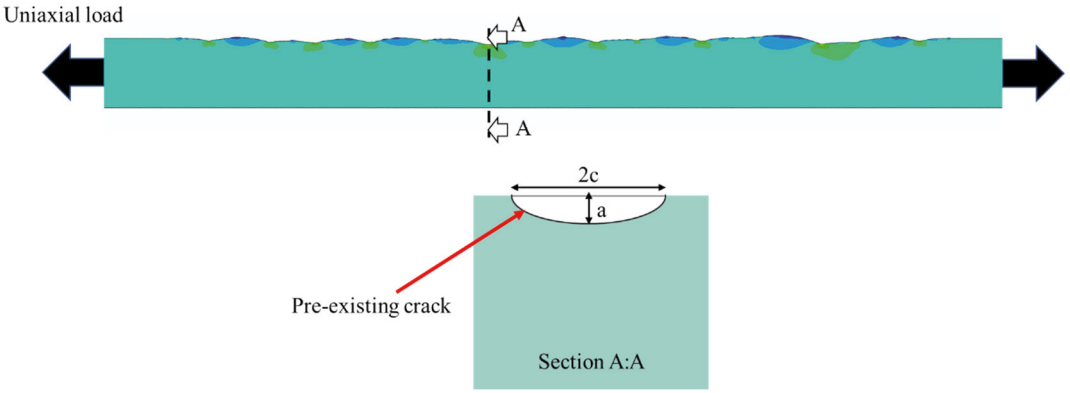

Figure 3: Schematic of an assumed pre-existing crack in a component with surface waviness (contours represent axial stress).

To describe the effect of the surface waviness on both short and long crack propagation, a unified model has been developed. The parameters of interest for this model are the new intrinsic short crack length a'_0, the critical crack length a'_D and the crack length dependent stress intensity factor range threshold $\Delta K'_a$. The influence of surface waviness on the unified model parameters is included as follows:

$$\Delta K_{th} = \gamma \Delta \sigma^R \sqrt{\pi (a + a_0^{'})} \tag{9}$$

Here $\Delta\sigma^R$ is the stress range threshold for a cracked component with surface waviness. This threshold should approach the fatigue limit of the specimen containing surface waviness ($\Delta\sigma_0^R$) for infinitely small cracks ($a \rightarrow 0$).

$$\lim_{a \to 0} \Delta \sigma^R = \Delta \sigma_0^R = \frac{\Delta K_{th}}{\gamma \sqrt{\pi a_0^{'}}} \tag{10}$$

Then, considering equation 11:

$$\Delta \sigma_0^R = \frac{\Delta K_{th}}{\gamma \sqrt{\pi a_0^{'}}} = \frac{\Delta \sigma_0}{K_t} \tag{11}$$

Hence, the new intrinsic short crack length a'_0 for a component with surface waviness is derived as:

$$a_0^{'} = \frac{1}{\pi} \left(\frac{K_t}{\gamma}\right)^2 \left(\frac{\Delta K_{th}}{\Delta \sigma_0}\right) \tag{12}$$

Analogous to the derivation of the modified El Haddad model (see equation 8), this crack length a'_0 is split up in the original material dependent crack length, similar to El Haddad intrinsic length a_0, and a new as-built critical defect length a'_D.

$$a_D^{'} = (\frac{K_t}{\gamma})^2 a_0 = K_t^2 a_D \tag{13}$$

The as-built crack length dependent stress intensity factor range threshold for specimens containing surface waviness ($\Delta K_a'$) can be defined as:

$$\Delta K_a^{'} = \Delta K_{th} \frac{\sqrt{a}}{\sqrt{a + a_D^{'}}} \tag{14}$$

As a short crack grows from the surface in the through thickness direction, the surface waviness threshold will achieve a steady state value equal to the crack propagation threshold for long cracks ΔK_{th}. As such, only the short crack propagation behavior will be affected by introducing these new modified parameters in the unified model. The effects of surface waviness on crack propagation behavior can thus be modelled by modifying the crack growth laws in the unified model. Along the surface direction, crack growth is modelled by imposing a stress field that is scaled linearly by a factor K_t. In the through thickness direction, the parameters of the short crack propagation model are modified to include surface waviness effects in the first stages of crack propagation. Inspired by Suraratchai et al. (2008), the unified model is described in the following twofold crack growth law:

$$\frac{da}{dN} = C_1(\Delta K - \Delta K_a^{'})^{m_1} \tag{15}$$

$$\frac{dc}{dN} = C_2(K_t \Delta K - \Delta K_a)^{m_2} \tag{16}$$

Note that for a smooth surface (K_t=1) equations 15 and 16 simplify to a conventional fatigue crack growth model with crack closure consideration.

In the unified model three parameters of the conventional short crack propagation model were modified to include surface waviness effects, a'_D, $\Delta K_a'$ and a'_0. Their immediate physical effects are twofold. The critical defect length a_D can be regarded as a measure of the crack growth that is needed before the crack length dependent threshold ΔK_{th} reaches the steady state value for long cracks ΔK_{th}. As a'_D is always larger than a_D, a component with surface waviness will require more crack growth before this steady state value is reached and transition to the long crack propagation regime occurs. The second effect is the influence of these parameters on the crack propagation rate (*da/dN*). As depicted in Fig.4, both thresholds (ΔK_a and $\Delta K_a'$) converge to ΔK_{th} after a certain crack growth, the propagation rates in the through thickness direction will be the same for a long crack originating from a smooth or from a rough surface (for cracks of equal size and driven by the same crack driving force).

To highlight the effect of the stress concentration factor arising from the surface waviness on the crack length dependent stress intensity factor range threshold ($\Delta K_a'$), a benchmark study has been conducted. In this study a pre-existing crack with a =30 µm and aspect ratio (*a/c*) of 0.5 has been assumed. This choice stems from the approximate grain size of the as-built component, and consequently the initial crack size should be well suited for the short crack regime. Given the similitude of a WAAM made component and a welded plate, a critical fracture toughness value of K_{Ic}=153 MPa was assumed from a study concerning fracture toughness in a high heat-input thick steel weld by An et al. (2014). From the surface profile measurements of different WAAM made components and the FE model described higher, three K_t values of 1.3 and 1.8 and 2.5 were extracted.

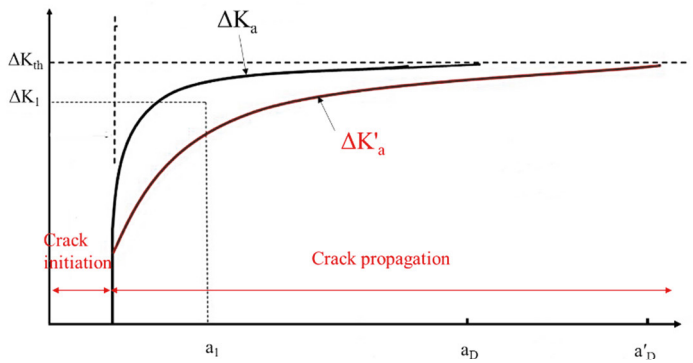

Figure 4: The influence of surface waviness critical defect length on the crack length dependent stress intensity factor range threshold.

Fig.5 demonstrates the crack length dependent stress intensity factor range threshold ($\Delta K_a'$) for various K_t values during the growth of the assumed pre-existing crack. It can be seen that as the crack grows, $\Delta K_a'$ converges toward the long crack threshold (ΔK_{th}). Chapetti (2003) suggested that for cracks larger than 20-30 times of the microstructural grain size, fully developed crack closure phenomenon and long crack propagation regime can be assumed. This range corresponds to a = 0.8-0.9 mm in the studied case, and Fig.5 indeed shows a negligible difference between the long crack threshold (dashed line in Fig. 5) and the smooth specimen threshold (blue line in Fig.5) at these values.

Fig. 5 also illustrates that the most pronounced influence of surface waviness can be found at the smaller crack length ranges. For cracks ranging between a =0.03 mm (the grain size) and a =0.3 mm (10 times the grain size), large differences can be observed between $\Delta K_a'$ and ΔK_{th}. Also, in this range K_t has the most significant effect on $\Delta K_a'$. This observation is of importance since it shows that, as a lower threshold leads to an increased propagation rate (see equation 15), higher surface waviness (larger K_t) increases the crack propagation rate of short cracks more significantly compared to that of relatively larger cracks.

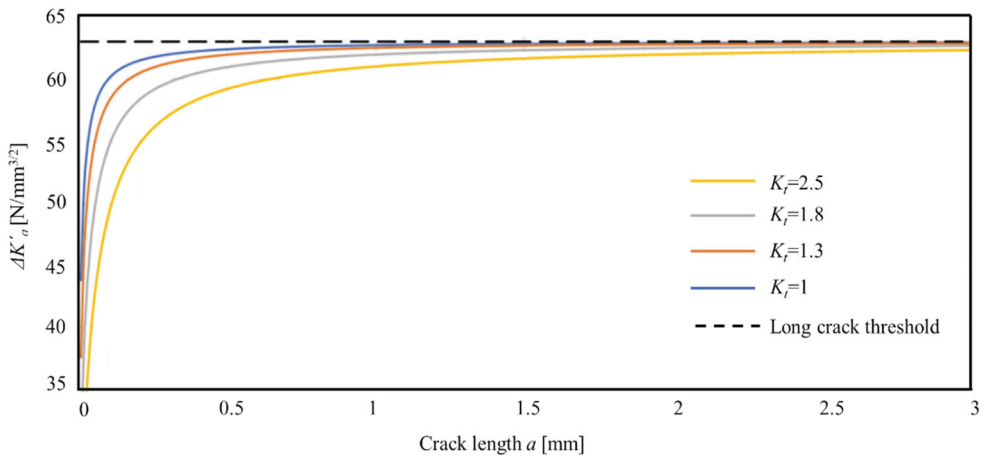

Figure 5: The influence of stress concentration factor (K_t) on the crack propagation threshold.

5. Conclusions

In this paper a model to incorporate the effect of surface waviness on short and long surface crack growth has been introduced. In this model, three parameters were modified to include surface waviness effects, the as-built intrinsic short crack length a'_0, the as-built critical defect length a'_D and the as-built crack length dependent stress intensity factor $\Delta K'_a$. This model has been developed based on El Haddad's short crack growth model, assuming the presence of an initial surface crack. This crack is assumed to grow both in through thickness and along surface directions and the stress concentration factor (K_t) influences both, yet by different mechanisms. As such, the crack size at which the short crack effect on crack propagation analysis diminishes, is increased when surface waviness is taken into consideration ($a'_D > a_D$). Consequently, the crack propagation rate (da/dN) is increased due to a reduced threshold of crack propagation. Therefore, in an as-built component with surface waviness, in both through thickness and in surface directions, not only a crack starts to grow faster than machined components with smooth surface, but it also grows at a faster rate. The driving force for crack growth along the surface direction is additionally enhanced due to the effect of K_t during the entire propagation period, while in through thickness direction the effect of K_t diminishes once the crack becomes larger than a threshold value. The unified model suggests that considering short crack regime in fatigue assessment of as-built WAAM components becomes more significant, since neglecting this step and only analyzing long crack growth, may lead to non-conservative predictions.

Acknowledgements

The authors acknowledge the financial support of Vlaio through the PrInt-AM project (HBC.2017.0613) and also the support by SIM (Strategic Initiative Materials in Flanders).

References

An, G.B., Woo, W., Park, J.-U., (2014). Brittle crack-arrest fracture toughness in a high heat-input thick steel weld. Int. J. Fract. 185, 179–185.

Arola, D., Williams, C.L., (2002). Estimating the fatigue stress concentration factor of machined surfaces. Int. J. Fatigue 24, 923–930.

Ås, S.K., Skallerud, B., Tveiten, B.W., (2008). Surface roughness characterization for fatigue life predictions using finite element analysis. Int. J. Fatigue 30, 2200–2209.

Chapetti, M.D., (2003). Fatigue propagation threshold of short cracks under constant amplitude loading. Int. J. Fatigue 25, 1319–1326.

Cunningham, C.R., Flynn, J.M., Shokrani, A., Dhokia, V., Newman, S.T., (2018). Invited review article: Strategies and processes for high quality wire arc additive manufacturing. Addit. Manuf. 22, 672–686.

Dirisu, P., Supriyo, G., Martina, F., Xu, X., Williams, S., (2020). Wire plus arc additive manufactured functional steel surfaces enhanced by rolling. Int. J. Fatigue 130, 105237.

Edwards, P., Ramulu, M., (2014). Fatigue performance evaluation of selective laser melted Ti-6Al-4V. Mater. Sci. Eng. A 598, 327–337.

El Haddad, M.H., Smith, K.N., Topper, T.H., (1979a). Fatigue crack propagation of short cracks. J. Eng. Mater. Technol. Trans. ASME 101, 42–46.

El Haddad, M.H., Smith, K.N., Topper, T.H., (1979b). Fatigue crack propagation of short cracks. J. Eng. Mater. Technol. Trans. ASME 101, 42–46.

Franco, L.A., Sinatora, A., (2015). 3D surface parameters (ISO 25178-2): Actual meaning of Spk and its relationship to Vmp. Precis. Eng. 40, 106–111.

Gong, H., Rafi, K., Gu, H., Starr, T., Stucker, B., (2014). Analysis of defect generation in Ti-6Al-4V parts made using powder bed fusion additive manufacturing processes. Addit. Manuf. 1, 87–98.

Irving, P.E., Beevers, C.J., (1974). Microstructural influences on fatigue crack growth in Ti-6Al-4V. Mater. Sci. Eng. 14, 229–238.

Kitagawa, H., Takahshi, S., (1976). Applicability of fracture mechanics to very small cracks or the cracks in the early stage. In: Proceddings of the Second International Conderance on Mechanical Behavior of Materials. Metals Park, OH, pp. 627–631.

Masuo, H., Tanaka, Y., Morokoshi, S., Yagura, H., Uchida, T., Yamamoto, Y., Murakami, Y., (2018). Influence of defects, surface roughness and HIP on the fatigue strength of Ti-6Al-4V manufactured by additive manufacturing. Int. J. Fatigue 117, 163–179.

Neuber, H., (1946). Theory of notch stresses: Principles for exact stress calculation. JW Edwards.

Novovic, D., Dewes, R.C., Aspinwall, D.K., Voice, W., Bowen, P., (2004). The effect of machined topography and integrity on fatigue life. Int. J. Mach. Tools Manuf. 44, 125–134.

Singh, K., Sadeghi, F., Correns, M., Blass, T., (2019). A microstructure based approach to model effects of surface roughness on tensile fatigue. Int. J. Fatigue 129, 105229.

Solberg, K., Guan, S., Razavi, S.M.J., Welo, T., Chan, K.C., Berto, F., (2019). Fatigue of additively manufactured 316L stainless steel: The influence of porosity and surface roughness. Fatigue Fract. Eng. Mater. Struct. 42, 2043–2052.

Stephens, R.I., Fatemi, A., Stephens, R.R., Fuchs, H.O., (2000). Metal fatigue in engineering. John Wiley & Sons.

Suraratchai, M., Limido, J., Mabru, C., Chieragatti, R., (2008). Modelling the influence of machined surface roughness on the fatigue life of aluminium alloy. Int. J. Fatigue 30, 2119–2126.

Taylor, D., (2008). The theory of critical distances. Eng. Fract. Mech. 75, 1696–1705.

Uzan, N.E., Shneck, R., Yeheskel, O., Frage, N., (2017). Fatigue of AlSi10Mg specimens fabricated by additive manufacturing selective laser melting (AM-SLM). Mater. Sci. Eng. A 704, 229–237.

Wycisk, E., Solbach, A., Siddique, S., Herzog, D., Walther, F., Emmelmann, C., (2014). Effects of defects in laser additive manufactured Ti-6Al-4V on fatigue properties. In: Physics Procedia. Elsevier B.V., pp. 371–378.

Yang, D., Liu, Z., Xiao, X., Xie, F., (2018). The effects of machining-induced surface topography on fatigue performance of titanium alloy Ti-6Al-4V. Procedia CIRP 71, 27–30.

Zhang, J., Fatemi, A., (2019). Surface roughness effect on multiaxial fatigue behavior of additive manufactured metals and its modeling. Theor. Appl. Fract. Mech. 103, 102260.